

Synthesis and Photophysical Studies of Chiral Helical Macrocyclic Scaffolds via Coordination-Driven Self-Assembly of 1,8,9,16-Tetraethynyltetraphenylenes. Formation of Monometallic Platinum(II) and Dimetallic Platinum(II)-Ruthenium(II) Complexes

Fang Lin,[†] Hai-Yan Peng,[†] Jing-Xing Chen,[†] David T. W. Chik,[‡] Zongwei Cai,[‡] Keith M. C. Wong,^{§,||} Vivian W. W. Yam,^{§,||} and Henry N. C. Wong*,^{†,||,⊥}

Shanghai-Hong Kong Joint Laboratory in Chemical Synthesis, Shanghai Institute of Organic Chemistry, The Chinese Academy of Sciences, 345 Ling Ling Road, Shanghai 200032, China, Department of Chemistry, Hong Kong Baptist University, Waterloo Road, Kowloon, Hong Kong SAR, China, Department of Chemistry, The University of Hong Kong, Pokfulam Road, Hong Kong SAR, China, and Institute of Molecular Functional Materials, Department of Chemistry, and Center of Novel Functional Molecules, The Chinese University of Hong Kong, Shatin, New Territories, Hong Kong SAR, China

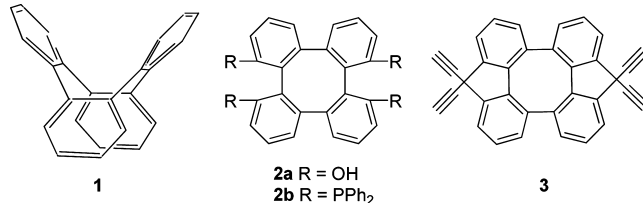
Received November 20, 2009; E-mail: hncwong@cuhk.edu.hk

Abstract: This paper is concerned with the synthesis and reactions of enantiopure 1,8,9,16-tetraethynyltetraphenylenes (**3**). We obtained **3** in 34% yield through four steps starting from 1,8,9,16-tetrahydroxytetraphenylenes (**2a**) via a functional group interconversion strategy. On the basis of this chiral “helical” building block, three rigid helical macrocycles **14**, **15**, and **22** were designed. Complexes **14** and **15** were constructed via coordination-driven self-assembly with platinum(II) complexes **8** and **9b**, while **22** cannot be obtained successfully. Then macrocycle **28** was designed on the structural basis of **22** to which octyl chains were introduced, in the hope of improving the solubility of the complex. Macrocycle **28** was finally formed and was characterized by NMR spectroscopy, elemental analysis, and electrospray mass spectrometry. For the enantiopure **15** and **28**, circular dichroism (CD) spectra also exhibited chiral properties. Complexes **27** and **28** both exhibited an intense emission band at 621 nm in acetonitrile at 298 K upon excitation at $\lambda > 420$ nm.

Introduction

Since the modestly efficient methods for the construction of tetraphenylenes (**1**) and its derivatives were recorded,^{1–3} considerable attention has been devoted to the design and syntheses of novel tetraphenylenes derivatives. Interest in this domain stems from the saddle shape geometry of **1** that should facilitate excellent three-dimensional dispositions crucial for the realization of helical frameworks,⁴ novel molecular clathrates,⁵ and asymmetric catalysts.^{3d} Due to the high barrier for inversion of the central cyclooctatetraene ring of **1**,^{3f} it is therefore of interest to prepare optically active tetraphenylenes derivatives which can

Scheme 1



be employed as chiral self-assembly building blocks for three-dimensional scaffolds.^{3a–e} We recently reported the synthesis of 1,8,9,16-tetrahydroxytetraphenylenes (**2a**), 1,8,9,16-tetrakis(diphenylphosphino)tetraphenylenes (**2b**) (Scheme 1), and the

* Shanghai Institute of Organic Chemistry, The Chinese Academy of Sciences.

† Hong Kong Baptist University.

‡ The University of Hong Kong.

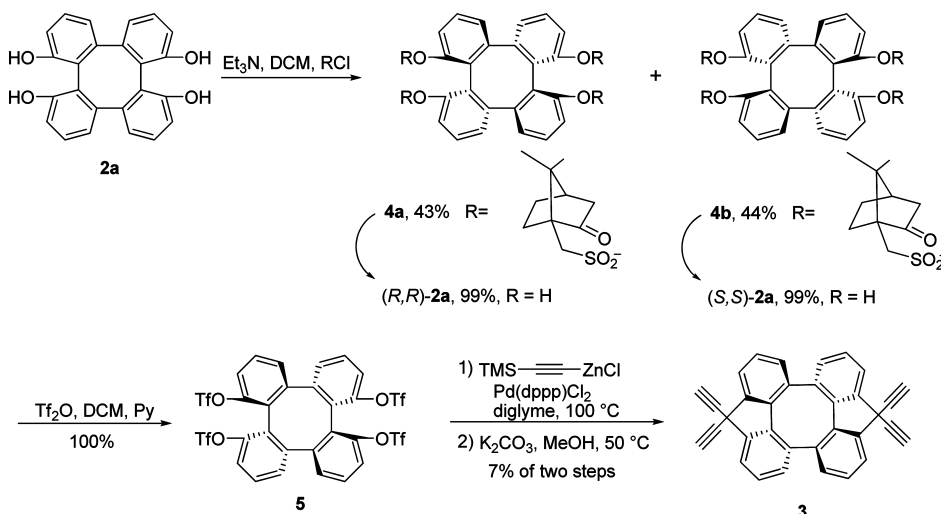
|| Institute of Molecular Functional Materials.

⊥ Department of Chemistry and Center of Novel Functional Molecules, The Chinese University of Hong Kong.

- (1) Rapson, W. S.; Shuttleworth, R. G.; van Niekerk, J. N. *J. Chem. Soc.* **1943**, 326–327.
- (2) For reviews, see: (a) Mak, T. C. W.; Wong, H. N. C. In *Comprehensive Supramolecular Chemistry*; MacNicol, D. D., Toda, F., Bishop, R., Eds.; Pergamon Press: Oxford, 1996; Vol. 6, pp 351–369. (b) Mak, T. C. W.; Wong, H. N. C. *Top. Curr. Chem.* **1987**, *140*, 141–164. (c) Huang, N. Z.; Sondheimer, F. *Acc. Chem. Res.* **1982**, *15*, 96–102. (d) Wong, H. N. C. *Acc. Chem. Res.* **1989**, *22*, 145–152.

- (3) (a) Wen, J.-F.; Hong, W.; Yuan, K.; Mak, T. C. W.; Wong, H. N. C. *J. Org. Chem.* **2003**, *68*, 8918–8931. (b) Lai, C. W.; Lam, C. K.; Lee, H. K.; Mak, T. C. W.; Wong, H. N. C. *Org. Lett.* **2003**, *5*, 823–826. (c) Hui, C. W.; Mak, T. C. W.; Wong, H. N. C. *Tetrahedron* **2004**, *60*, 3523–3532. (d) Peng, H.-Y.; Lam, C.-K.; Mak, T. C. W.; Cai, Z. W.; Ma, W.-T.; Li, Y.-X.; Wong, H. N. C. *J. Am. Chem. Soc.* **2005**, *127*, 9603–9611. (e) Wu, A.-H.; Hau, C.-K.; Wong, H. N. C. *Adv. Synth. Catal.* **2007**, *349*, 601–608. (f) Bachrach, S. M. *J. Org. Chem.* **2009**, *74*, 3609–3611. (g) Huang, H.; Stewart, T.; Gutmann, M.; Ohhara, T.; Niimura, N.; Li, Y.-X.; Wen, J.-F.; Bau, R.; Wong, H. N. C. *J. Org. Chem.* **2009**, *74*, 359–369. (h) Huang, H.; Hau, C.-K.; Law, C. C. M.; Wong, H. N. C. *Org. Biomol. Chem.* **2009**, *7*, 1249–1257.

Scheme 2



chiral rodlike platinum complexes employing **2a** and **2b** as building blocks.^{3d} As compared with **2a** and **2b**, 1,8,9,16-tetraethynyltetraphenylenes (**3**) is more helical-like because the introduction of ethynyl groups on C-1, C-8, C-9, and C-16 renders **3** an excellent candidate for constructing rigid helical supermolecules.

Coordination-driven self-assembly of supramolecular scaffolds such as sticks, squares, helices, cylinders, and cages have significantly grown over the past decade.⁶ Compared to covalently bonded organic counterparts, the preparation of metal–organic supermolecules enjoys higher efficiency and ease after elaborate designs. Herein, we wish to report an efficient synthesis of **3** as well as the realization of a series of enantiopure helical macrocycles containing the structural motif of **3**. We believe that such helical macrocycles possess attractive potential applications as luminescent and nonlinear optical materials, molecular wires, and molecular electronics, because of the alkynyl group's inherent property of linear geometry, structural rigidity, π -electron delocalization, and ability to interact with metal via $\text{p}\pi-\text{d}\pi$ overlap.⁷ It is noteworthy that **3** can also transfer its chirality to the macrocycle cores, which make the macrocycles possess optical rotation values.⁸ To the best of our

knowledge, there have been no literature reports on macrocycles that are assembled by enantiopure tetraphenylenes derivatives.

Results and Discussion

Synthesis of Enantiopure 1,8,9,16-Tetraethynyltetraphenylenes (3**).** Appropriate substituents on C-1, C-8, C-9, and C-16 on tetraphenylenes (**1**) endow **1** superior potential as a rigid building block in the formation of helical macrocycles. Nonetheless, the steric hindrance on these positions due to the molecular shape also leads to the difficulty in realizing **3**. Enantiopure **2a** was prepared by resolution through (*S*)-camphorsulfonylation.^{3d} Due to the defined absolute configuration of the (*S*)-camphorsulfonyl group, enantiomerically pure (*S,S*)-**2a** and (*R,R*)-**2a** were obtained after subsequent desulfonylation steps. With enantiopure **2a** in hand, enantiopure **3** was primarily obtained by transition metal coupling reactions. Due to the steric hindrance of the tetraphenylenes scaffold, triflate **5** failed to react with trimethylsilylacetylene under the conditions of Sonogashira⁹ and Kumada reactions.¹⁰ In these attempts, starting material **5** was recovered. We then switched our efforts to a Negishi reaction,¹¹ since zinc reagents should be more reactive. Trimethylsilyl-ethynyl zinc chloride did react with triflate **5** catalyzed by $\text{Pd}(\text{dppp})\text{Cl}_2$ in diglyme at 100 °C. Without further purification, trimethylsilyl groups were removed by K_2CO_3 in MeOH (Scheme 2). After careful chromatography, **3** was separated in a disappointing yield of only 7%, which was too low to fulfill the next step for the synthesis of macrocycles. In this procedure, products with two remaining triflic groups were also detected. These results indicate that the Negishi reaction was by no means efficient for the introduction of ethynyl groups to the sterically compact tetraphenylenes molecule.

We therefore directed our attention to the use of cyano groups instead of a trimethylsilyl-ethynyl group, as the former has a

- (4) (a) Rajca, A.; Safronov, A.; Rajca, S.; Shoemaker, R. *Angew. Chem., Int. Ed. Engl.* **1997**, *36*, 488–491. (b) Marsella, M. J.; Kim, I. T.; Tharn, F. *J. Am. Chem. Soc.* **2000**, *122*, 974–975.
- (5) Man, Y.-M.; Mak, T. C. W.; Wong, H. N. C. *J. Org. Chem.* **1990**, *55*, 3214–3221.
- (6) For reviews, see: (a) Leininger, S.; Olenyuk, B.; Stang, P. J. *Chem. Rev.* **2000**, *100*, 853–907. (b) Seidel, S. R.; Stang, P. J. *Acc. Chem. Res.* **2002**, *35*, 972–983. (c) Swiegers, G. F.; Malefetse, T. J. *Coord. Chem. Rev.* **2002**, *225*, 91–121. (d) Holliday, B. J.; Mirkin, C. A. *Angew. Chem., Int. Ed.* **2001**, *40*, 2022–2043. (e) Cotton, F. A.; Lin, C.; Murillo, C. A. *Acc. Chem. Res.* **2001**, *34*, 759–771. (f) Fujita, M. *Chem. Soc. Rev.* **1998**, *27*, 417–425. (g) Lee, S. J.; Lin, W. *Acc. Chem. Res.* **2008**, *41*, 521–537. (h) Schwab, P. F. H.; Levin, M. D.; Michl, J. *Chem. Rev.* **1999**, *99*, 1863–1934. (i) Fujita, M.; Tominaga, M.; Hori, A.; Therrien, B. *Acc. Chem. Res.* **2005**, *38*, 369–378. (j) Ward, M. D. *Chem. Commun.* **2009**, 4487–4499.
- (7) (a) Ziessel, R.; Hissler, M.; Elghayoury, A.; Harriman, A. *Coord. Chem. Rev.* **1998**, *178–180*, 1251–1298. (b) Khan, M. S.; Kakkar, A. K.; Long, N. J.; Lewis, J.; Raithby, P. R.; Marder, T. B.; Wittmann, F.; Friend, R. H. *J. Mater. Chem.* **1994**, *4*, 1227–1232. (c) Yam, V. W.-W.; Yu, K.-L.; Wong, K. M.-C.; Cheung, K.-K. *Organometallics* **2001**, *20*, 721–726. (d) Yam, V. W.-W. *Acc. Chem. Res.* **2002**, *35*, 555–563. (e) Yam, V. W.-W.; Wong, K. M.-C.; Zhu, N. Y. *J. Am. Chem. Soc.* **2002**, *124*, 6506–6507. (f) Yam, V. W.-W.; Wong, K. M.-C.; Zhu, N. Y. *Angew. Chem., Int. Ed.* **2003**, *42*, 1400–1403. (g) Yam, V. W.-W.; Chan, K. H.-Y.; Wong, K. M.-C.; Chu, B. W.-K. *Angew. Chem., Int. Ed.* **2006**, *45*, 6169–6173.
- (8) (a) Katz, T. J. *Angew. Chem., Int. Ed.* **2000**, *39*, 1921–1923. (b) Graule, S.; Rudolph, M.; Vanthuyne, N.; Autschbach, J.; Roussel, C.; Crassous, J.; Réau, R. *J. Am. Chem. Soc.* **2009**, *131*, 3183–3185.
- (9) (a) Sonogashira, K.; Tohda, Y.; Hagiwara, N. *Tetrahedron Lett.* **1975**, *16*, 4467–4470. For review, see: (b) Hegedus, L. S. *J. Organomet. Chem.* **1993**, *457*, 167–272. (c) Alami, M.; Linstrumelle, G. *Tetrahedron Lett.* **1991**, *32*, 6109–6112.
- (10) Tamao, K.; Sumitani, K.; Kumada, M. *J. Am. Chem. Soc.* **1972**, *94*, 4374–4375.
- (11) (a) King, A. O.; Okukado, N.; Negishi, E. *J. Chem. Soc., Chem. Commun.* **1977**, 683–684. (b) Negishi, E.; Okukado, N.; King, A. O. *J. Am. Chem. Soc.* **1978**, *100*, 2254–2255.

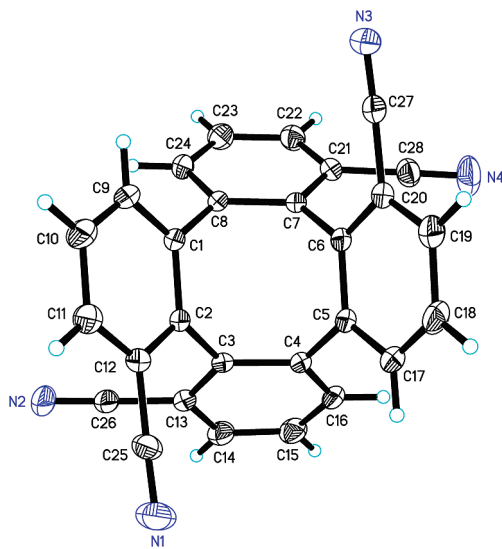
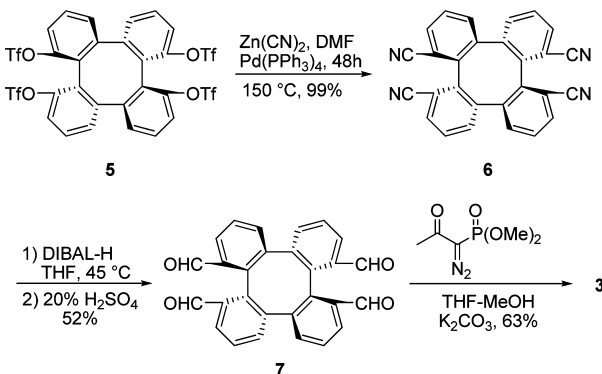


Figure 1. ORTEP drawing of **6**.

Scheme 3



much smaller bulk than the latter and, as a result, could probably reduce the influence of steric hindrance for palladium catalyst coupling reaction. Nitrile **7** could be converted to **3** by using a functional group interconversion strategy. In order to introduce cyano groups to triflate **5**, a protocol established by Rice was employed.¹² Under the conditions of Pd(PPh₃)₄, Zn(CN)₂, and anhydrous DMF, with heating at 150 °C for 2 days, we were able to achieve the isolation of 1,8,9,16-tetracyanotetraphenylene (**6**) in an almost quantitative yield (Figure 1). The crucial key to this success was to keep the reaction under absolutely anhydrous conditions. Compound **6** exhibited strong signals at *m/z* 404 in its mass spectrum. ¹H NMR, elemental analysis, and X-ray crystallographic results also supported the structure of **6**. Subsequently, **6** was reduced by DIBAL-H at 45 °C and was followed by acidification with 20% sulfuric acid. In this way, tetraphenylene-1,8,9,16-tetraal (**7**) was obtained in a moderate yield.¹³ Its ¹H NMR spectra (300 MHz, CDCl₃) exhibited a singlet at δ 9.53 ppm that can be assigned to the four aldehyde protons. Eventually, reaction of **7** with the Bestmann reagent¹⁴ allowed its direct conversion to **3** in 63% yield. Compound **3** exhibited a singlet at δ 2.85 ppm that can be assigned to terminal ethynyl protons. Moreover, the molecular ion peak of **3** in its

- (12) Kubota, H.; Rice, K. C. *Tetrahedron Lett.* **1998**, *39*, 2907–2910.
 (13) Miller, A. E. G.; Biss, J. W.; Schwartzman, L. H. *J. Org. Chem.* **1959**, *24*, 627–630.
 (14) (a) Müller, S.; Liepold, B.; Roth, G. J.; Bestmann, H. J. *Synlett* **1996**, 521–522. (b) Roth, G. J.; Bernd, L.; Müller, S. G.; Bestmann, H. J. *Synthesis* **2004**, 59–62.

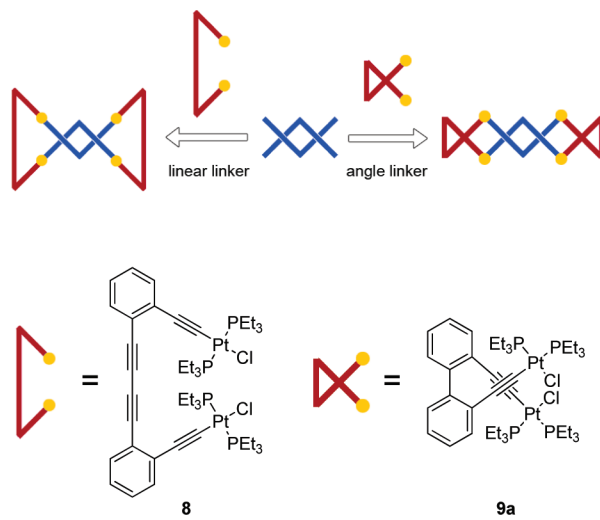
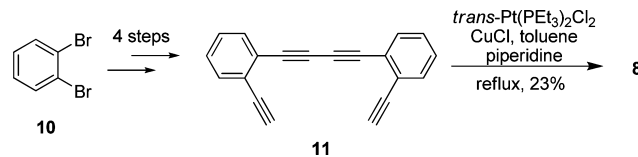


Figure 2. Linear linker **8** and the angle linker **9a**.

Scheme 4



EI mass spectrum was observed at *m/z* 400.1250, which is in good agreement with the theoretical value of 400.1252 for the molecular formula C₃₂H₁₆ of **3**. By utilizing a sequential functional group transformation route as shown in Scheme 3, we then prepared both enantiopure (*S,S*)-**3** and (*R,R*)-**3** in 34% yield starting from enantiopure (*S,S*)-**2a** and (*R,R*)-**2a**, respectively.

Synthesis of Platinum(II) Complexes **8 and **9b**.** In light of the inherent rigidity and helicity of **3**, it was anticipated that the tectons self-assembled with **3** should adhere strictly to the directional-bonding methodology,^{6b,d} and also a relatively flexible structure was necessary. Then the rigidity and chirality can be transferred through **3** to the whole macrocycles after self-assembly.¹⁴ Herein we designed two types of ditopic metal containing tectons to link with **3**, i.e. the linear linker **8** and the angle linker **9a** that are shown in Figure 2. Platinum(II) alkynyl complexes were designed taking account their robust abilities of constructing well-defined finite supramolecular structures and potential electrochemical, photochemical, and optoelectronic properties.⁷

With enantiopure **3** in hand, our target therefore was to synthesize the platinum complex **8** and **9a** and to connect them with **3** via coordination-driven self-assembly protocol. The preparation of **8** is outlined in Scheme 4. **11** was prepared according to the literature.¹⁶ The resulting 1,4-bis[2-*trans*-Pt(PEt₃)₂Cl]phenylbutadiyne **8** was obtained by reacting **11** with 2 equiv of *trans*-Pt(PEt₃)₂Cl₂ in the presence of a CuCl catalyst in a 1:1 mixture of toluene/piperidine at 100 °C. The structure of tecton **8** was confirmed by elemental analysis, ¹H, ¹³C{¹H}, ³¹P{¹H} NMR, IR spectroscopy, mass spectrometry, and X-ray crystallographic analysis. Four equivalent phosphorus atoms in **8** gave rise to a sharp singlet at 16.2 ppm in the ³¹P{¹H} spectra (121.5 MHz, CDCl₃), with a set of ¹⁹⁵Pt satellites (¹J_{Pt-P} = 2378 Hz). The geometry around each Pt is close to a square planar geometry (Figure 3).

The synthesis of **9a** was shown in Scheme 5. In our previous design, starting from phenanthrene **12**, through three steps,^{17,14}

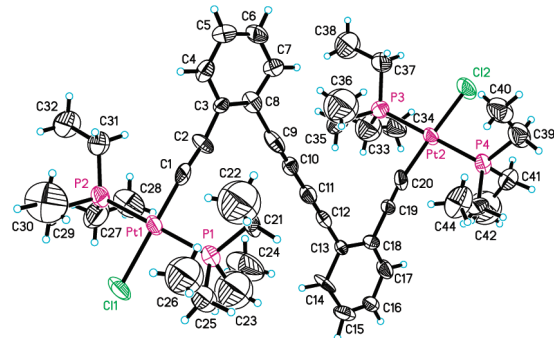
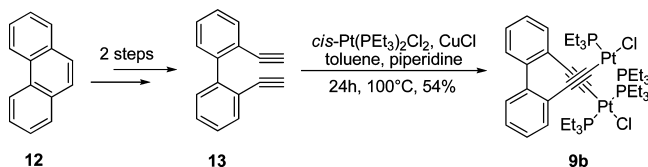


Figure 3. ORTEP drawing of **8**.

Scheme 5



cis-[Pt₂(bipy)(PEt₃)₄Cl₂]₂ (**9a**) was prepared by using 2 equiv of *cis*-Pt(PEt₃)₂Cl₂. However, neither the CuCl catalyzed conditions employing toluene/piperidine as solvents with heating^{18a} nor milder conditions using THF/Et₂NH at room temperature^{18b,c} gave the corresponding *cis*-complex. It was found that only *trans*-[Pt₂(bipy)(PEt₃)₄Cl₂]₂ **9b** was obtained, whose structure was supported by an X-ray diffraction study (Figure 4). The isolation of the resulting *trans*-isomer **9b** indicates that the *cis*-isomer **9a** is not kinetically stable and unable to resist a thermal or a photochemical isomerization. This result was unexpected, as the *trans*-isomer **9b** does not possess the appropriate conformation of the designed macrocycle.

Self-Assembly and Characterization of Platinum(II) Complexes 14 and 15. The self-assembly of macrocycle **14** and **15** is outlined in Scheme 6 using a typical procedure (Figure 5).¹⁹ In the formation of macrocycle **14**, complex **8** was unable to react completely, 60% of which was recovered, while, in the formation of macrocycle **15**, complex **9b** was able to react completely according to a TLC study. In the process of workup, both reactions demonstrated a similar phenomenon; i.e. when the reaction solvent was removed directly under vacuum, a

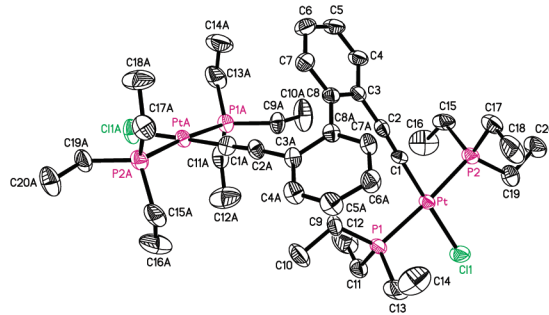


Figure 4. ORTEP drawing of **9b**.

semitransparent oil resulted in the reaction flask. After diluting this oil with CH₂Cl₂, a semitransparent thin film formed, whose solubility was too low that it is practically insoluble in almost all organic solvents, even under heating. However, if CH₂Cl₂ was utilized to dilute the reaction mixture, and the organic layer was washed consecutively by water and aqueous NH₄Cl to remove CuCl and the base, macrocycles **14** and **15** with good solubility were obtained respectively after the removal of solvents in vacuum.

The solubility of the aforementioned thin films was so low that their identification by NMR and mass spectra was impossible. Notwithstanding, from the limited evidence of elemental analysis and the IR spectrum,²⁰ we anticipate that cross-linking products were formed, whose specific structures are still unknown.

NMR analysis of the soluble products indicated formation of the target macrocyclic species. There are only signals of protons on the aromatic rings and PEt₃ ligands in both ¹H NMR spectra of macrocycles **14** and **15**. The ³¹P{¹H} NMR spectrum of **14** showed two sharp singlets at 12.7 and 15.8 ppm, both with a set of ¹⁹⁵Pt satellites (¹J_{Pt-P} = 2389 and 2397 Hz), respectively, which was similar to the ³¹P{¹H} NMR spectrum of **15**. The two sharp phosphorus singlets suggested that there were two different phosphorus atoms in **14** or **15**, which can be explained as the transfer of rigidity from **3** to the whole macrocycles so that the two PEt₃ ligands were fixed and therefore differentiated.

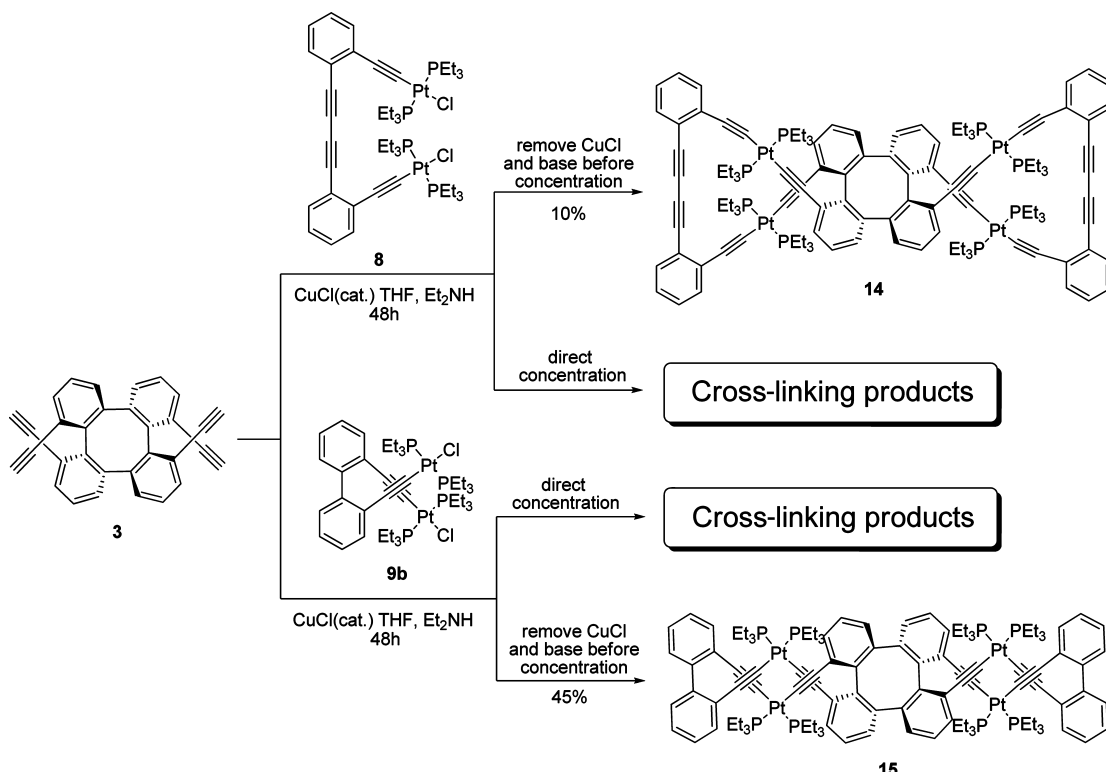
ESI-MS spectra further substantiated the formation of these two macrocycles. The ESI mass spectrum gave the (M + H)⁺ peak, with an *m/z* ratio of 2617.7992 (calcd 2617.8152) for **14**. As for macrocycle **15**, the (M + K)⁺ peak, *m/z* = 2559.7539 (calcd 2559.7711) was observed. Elemental analysis results also confirmed the proposed structures.

The poor yield of **14** can be explained by the following observation. When the X-ray structure of **9b** is compared with that of **8**, there is a 120.83° dihedral angle existing in the biphenyl backbone. While, in structure **8**, the two Pt (II) moieties are almost opposite to each other and the backbone is in a plane (Figure 6). That means complex **8** needs more energy than **9b** to distort to a proper dihedral angle in order to fit the rigid **3**.

For the formation of **15**, we supposed that, after a long period of reaction time, the two components connect to each other by metal–carbon covalent bonds in a certain style, which is a dynamic stable state in a dilute solution.²¹ In such a self-assembly system, bonding processes are reversible and the formation of products are in continuous equilibrium, just like many supramolecular systems with “error-checking” or “proof-reading” properties,²² that ensures the eradication of thermodynamically unstable products. However, a change in

- (15) (a) Anderson, S.; Neidlein, U.; Gramlich, F.; Diederich, F. *Angew. Chem., Int. Ed. Engl.* **1995**, *34*, 1596–1600. (b) Bähr, A.; Droz, A. S.; Pünter, M.; Neidlein, U.; Anderson, S.; Seiler, P.; Diederich, F. *Helv. Chim. Acta* **1998**, *81*, 1931–1963. (c) Droz, A. S.; Diederich, F. *J. Chem. Soc., Perkin Trans. 1* **2000**, 4224–4226.
- (16) Hay, A. S. *J. Org. Chem.* **1962**, *27*, 3320–3321.
- (17) Bailey, P. S.; Erickson, R. E.; Caserio, M. C.; Roberts, J. D. *Org. Synth. Coll. Vol. 5* **1973**, 489–492.
- (18) (a) Ohshiro, N.; Takei, F.; Onitsuka, K.; Takahashi, S. *J. Organomet. Chem.* **1998**, *569*, 195–202. (b) Onitsuka, K.; Yamamoto, S.; Takahashi, S. *Angew. Chem., Int. Ed.* **1999**, *38*, 174–176. (c) Lee, S. J.; Hu, A.; Lin, W. *J. Am. Chem. Soc.* **2002**, *124*, 12948–12949.
- (19) Procedures: a dilute solution of **3** and 2 equiv of either Pt(II) complex **8** or **9b** in a 1:1 mixture of THF/Et₂NH was stirred for about 48 h in a catalytic amount of CuCl at room temperature, until **3** was completely consumed.
- (20) The resulting thin film formed from **3** and **9b** showed that the element contents (C, 49.82; H, 6.14) were very close to those values of a complex formed from 4 mol of complex **9b** linking with 1 mol of **3** (C, 49.61; H, 6.16). As expected, the IR spectrum showed the disappearance of ν (C≡C–H) stretches at \sim 3286 cm^{−1} and the appearance of strong ν (C≡C) stretches at \sim 2090 cm^{−1}.
- (21) Rowan, S. J.; Cantrill, S. J.; Cousins, G. R. L.; Sanders, J. K. M.; Stoddart, J. F. *Angew. Chem., Int. Ed.* **2002**, *41*, 898–952.

Scheme 6



external factors, such as concentration, catalyst, pressure, and temperature, etc., can have a dramatic effect upon the equilibrium and therefore change the product distribution, even though the initial product has formed. As for our self-assembly systems, the condensation of solution led to the collapse of the equilibrium, which resulted in the irreversible formation of cross-linking products. On the other hand, the

removal of the catalyst (CuCl) also disturbed the balance of the system, and macrocycles were therefore generated.

Synthesis and Characterization of Platinum(II)–Ruthenium(II) Dimetallic Complex. The synthesis of **14** and **15** prompted us to undertake a more challenging synthesis of another rigid helical macrocycle in which bipyridine moieties were introduced as second metal binding sites, leading to coordination with a second



Figure 5. Ball-and-stick model of **14** and **15** (Chem3D).

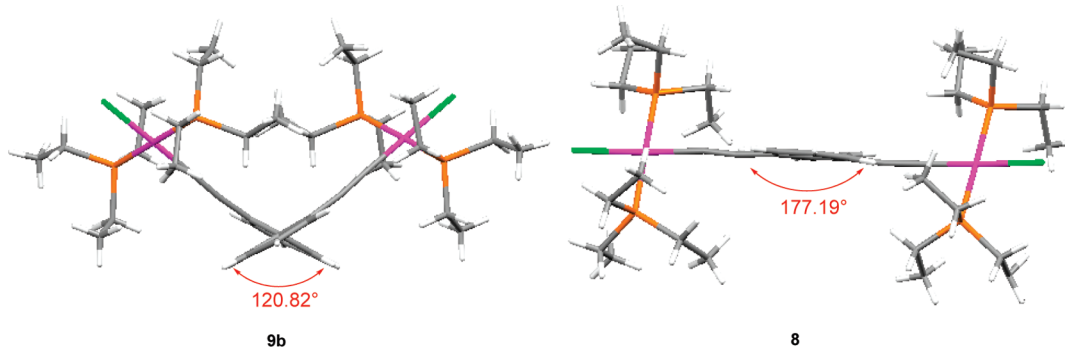


Figure 6. Capped sticks models of **9b** and **8**.

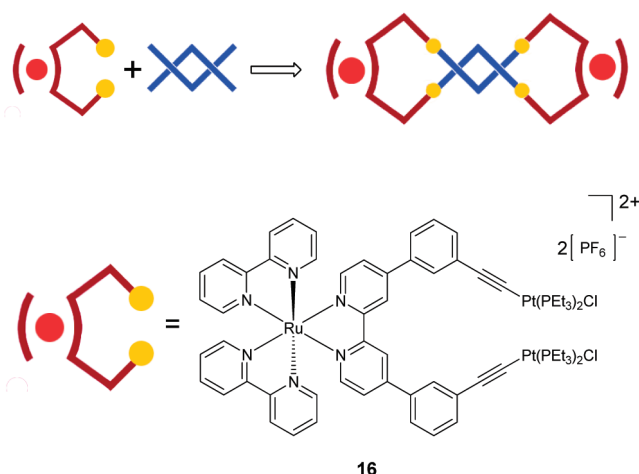


Figure 7. Synthesis of a rigid helical macrocycle in which bipyridine moieties were introduced as second metal binding sites utilizing complex 16

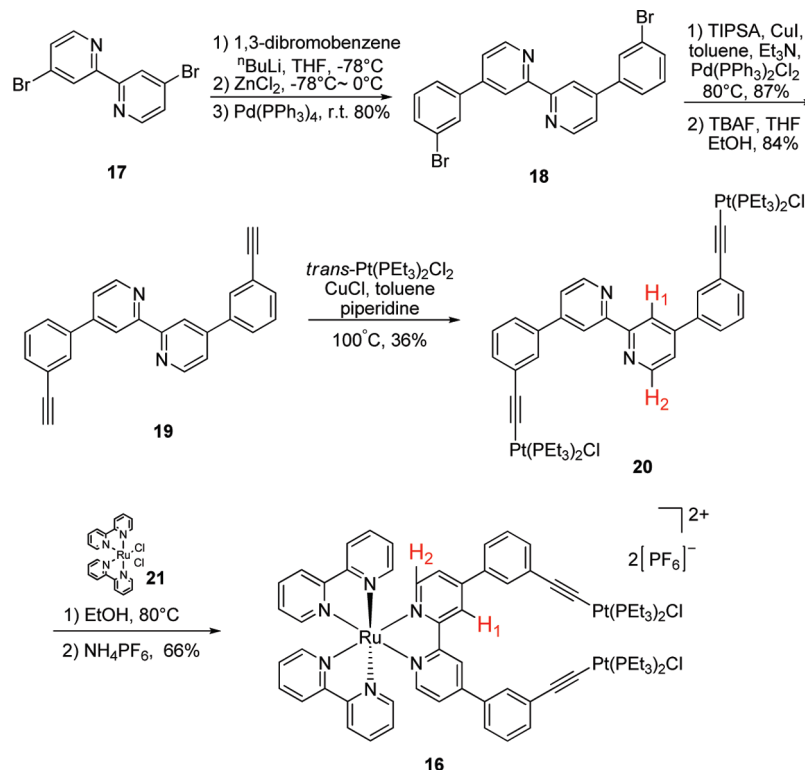
metal in an intermolecular manner (Figure 7). Dimetallic complex **16** was accordingly designed for this purpose. The synthesis of **16** from 4,4'-dibromo-2,2'-bipyridine **17** was accomplished in five steps (Scheme 7). Complex **20** was allowed to react with *cis*-Ru(bpy)₂Cl₂ **21** in EtOH, which was followed by treatment with aqueous NH₄PF₆ solution, affording complex **16** in a moderate yield. In the ¹H NMR spectrum (300 MHz, CDCl₃) of **20**, the width between proton H₁ and H₂ was just 0.03 ppm, while, in that of complex **16** (300 MHz, acetone-*d*₆),²³ the signal of H₁ was shifted dramatically to low field and the corresponding width increased to 0.43 ppm. This phenomenon can be explained by the fact that the four aryl rings in **16** experienced a deshielding effect on H₁ after coordinating with Ru(II). These data are consistent with the expected structure of

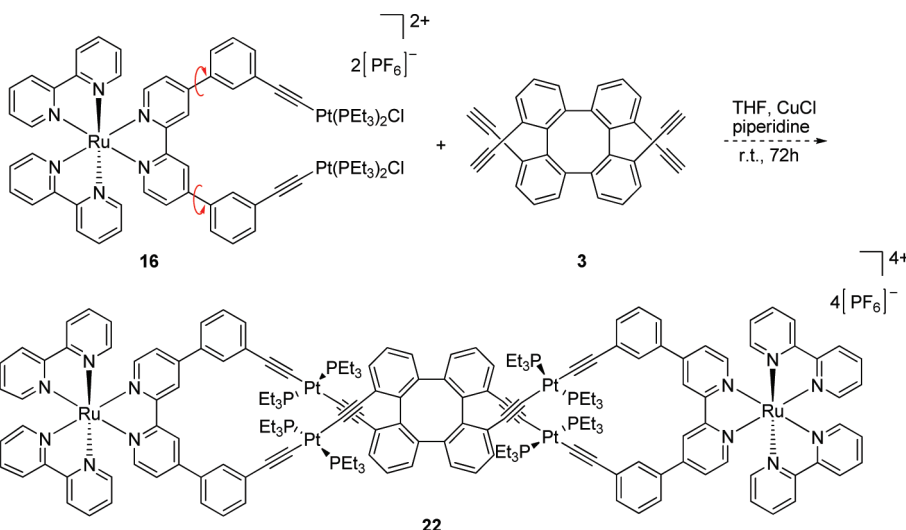
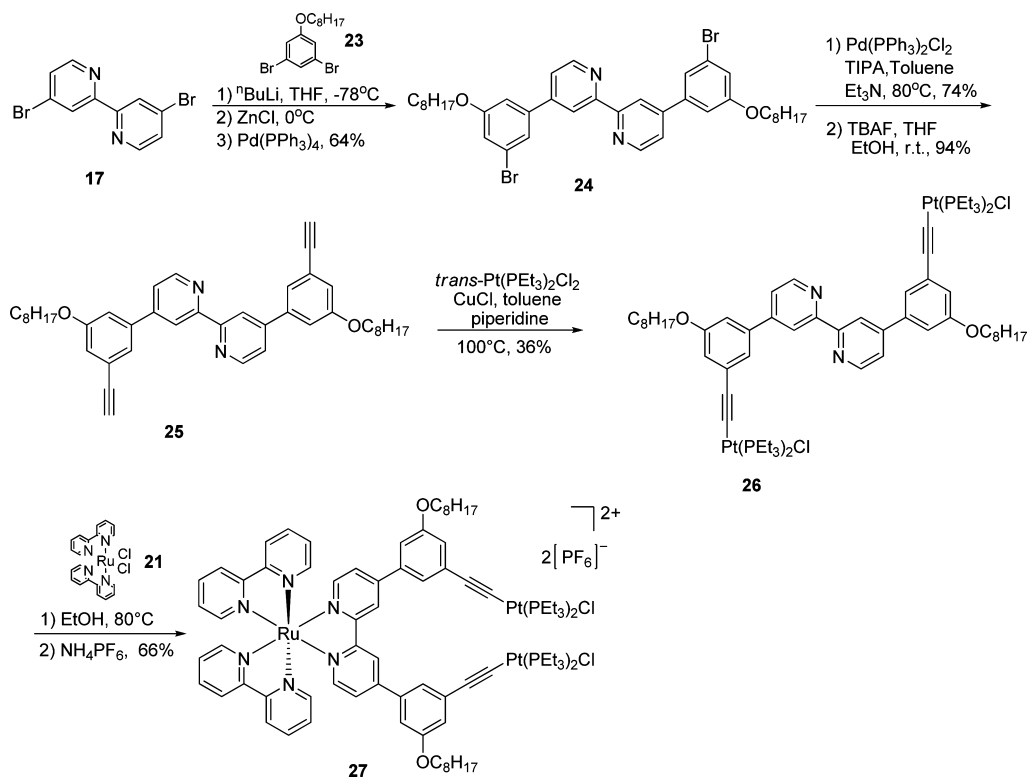
16, which is also supported by elemental analysis, $^{13}\text{C}\{^1\text{H}\}$, $^{31}\text{P}\{^1\text{H}\}$ NMR, and IR spectroscopy.

With complex **16** and tetraethynyltetraphenylenes **3** in hand, we then explored the potential of the self-assembly to form macrocycle **22**. But unfortunately, the method used for the synthesis of macrocycles **14** and **15** unexpectedly failed for **22**. A red precipitate was generated whose solubility was too low to be identified. The ^1H NMR spectra (300 MHz, acetone- d_6) of this precipitate indicated that the signal of ethynyl proton disappeared, while only signals of aromatic rings and PEt₃ ligands were found. The $^{31}\text{P}\{^1\text{H}\}$ NMR spectra (121.5 MHz, acetone- d_6) showed two sharp singlets which were similar to those observed for **14** and **15**. However, the results of the mass spectrum and elemental analysis were unable to substantiate the nature of this macrocycle. When (*S,S*)-**3** and (*R,R*)-**3** respectively were used in the same method to assemble with **16**, the corresponding products with opposite specific rotation and reversed circular dichroism (CD) spectra were observed, which indicated that chiral **3** did connect with **16** in a certain unknown manner rather than the predesigned one. We supposed that the bonds connecting bipyridine and the benzene ring could rotate randomly, which was unfavorable for the self-assembly of **22** (Scheme 8). This unsuccessful attempt inspired us to make a partial modification on the Ru(II)–Pt(II) bipyridine building block **16**.

Octyl chains were introduced into **16** to form compound **27**, on account of improving the solubility of the self-assembly products. In this way, the two acetylenic Pt(II) reacting positions can be fixed to some extent, as the introduction of the long aliphatic chains can somehow restrict the random bond rotation between bipyridine and the benzene ring. The synthesis of **27** was accomplished in five steps by the aforementioned methods with a moderate yield (Scheme 9) and was unequivocally

Scheme 7



Scheme 8**Scheme 9**

characterized by ^1H , $^{13}\text{C}\{^1\text{H}\}$, $^{31}\text{P}\{^1\text{H}\}$ NMR, IR spectroscopy, and ESI-MS spectrometry.

With complex **27** and **3** in hand, we then explored the self-assembly of macrocycle **28** (Figure 8). To a dilute solution of **3** in a 15:1 mixture of THF/piperidine was added a solution of **27** in THF in a dropwise manner (Scheme 10). Then the resulting red solution was stirred at room temperature for 3 days until a product with high polarity formed. After the workup process, a leaf-shaped red solid was obtained with good solubility in acetone and acetonitrile. The structure of macrocycle **28** was therefore substantiated by ESI-MS spectrometry,

which gave $(\text{M}-3\text{PF}_6)^{3+}$ and $(\text{M}-4\text{PF}_6)^{4+}$ peaks, with respective m/z ratios of 1438.4879 and 1042.6286. The $(\text{M}-\text{PF}_6)^+$ peak of **28** ($m/z = 4605.4$) was out of the range of the spectrometer. The ^1H NMR, $^{31}\text{P}\{^1\text{H}\}$ NMR, and IR spectra were consistent with structure **28**. Also the elemental analysis results [C, 51.21; H, 6.00; N, 3.49 (calcd C, 51.58; H, 5.63; N, 3.54)] confirmed the proposed molecular formula.

- (23) Complex **16** is just slightly soluble in CDCl_3 but soluble in acetone- d_6 . The ^1H NMR spectrum of **16** shows that the protons of **16** have a similar chemical shift in both CDCl_3 and acetone- d_6 .
- (24) (a) Masai, H.; Sonogashira, K.; Hagihara, N. *Bull. Chem. Soc. Jpn.* **1971**, *44*, 2226–2230. (b) Sacksteder, L.; Baralt, E.; DeGraff, B. A.; Lukehart, C. M.; Demas, J. N. *Inorg. Chem.* **1991**, *30*, 2468–2476. (c) Choi, C. L.; Cheng, Y. F.; Yip, C.; Phillips, D. L.; Yam, V. W. W. *Organometallics* **2000**, *19*, 3192–3196.

(22) Fang, Y.-Q.; Polson, M. I. J.; Hanan, G. S. *Inorg. Chem.* **2003**, *42*, 5–7.

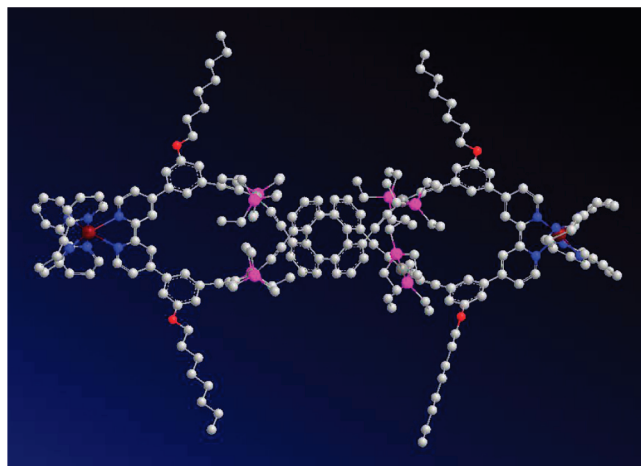


Figure 8. Ball-and-stick model of **28** (Chem3D).

(*S,S*)-**3** and (*R,R*)-**3** were used to form the enantiomeric compounds of **15** and **28** respectively. The CD spectrum of **28**, **15**, and **3** are shown in Figure 9. Metallocycle **15** exhibited one major band and two minor bands with a red shift in energy and higher intensities as compared with compound **3**. The CD spectra of **28** exhibited one major band and one minor band with much higher intensities as compared with **3** and macrocycle **15**, which indicates the occurrence of chiral properties during the self-assembly processes.

Photophysical Properties. The electronic absorption spectra of selected compounds are shown in Figure 10, and their photophysical data are summarized in Table 1. Alkyne **3** showed a high-energy absorption band at about 246–254 nm, which is attributed to the $\pi-\pi^*$ transition. The dinuclear alkynylplatinum(II) complex **9b** exhibited higher-energy absorption bands at 246–278 nm and lower-energy absorption bands at 300–320 nm. In view of the spectroscopic studies on the alkynylplatinum(II) phosphine complexes,²⁴ the higher-energy absorption bands are assigned as a $\pi-\pi^*$ intraligand (IL) transition of the alkynyl linker **13**, while the lower-energy absorption bands are ascribed to the admixture of $\pi-\pi^*$ IL and $d\pi(\text{Pt}) \rightarrow \pi^*(\text{C}\equiv\text{CR})$

Scheme 10

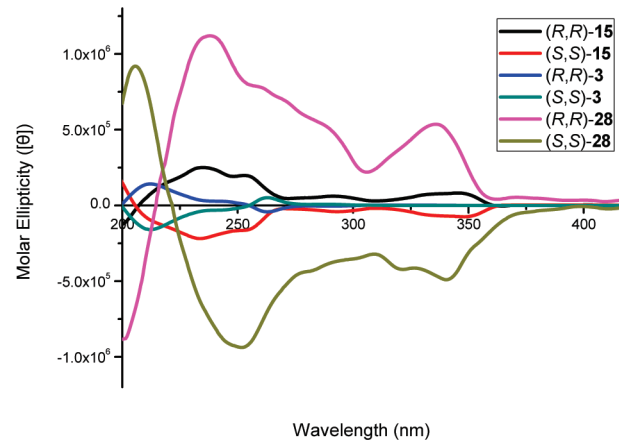
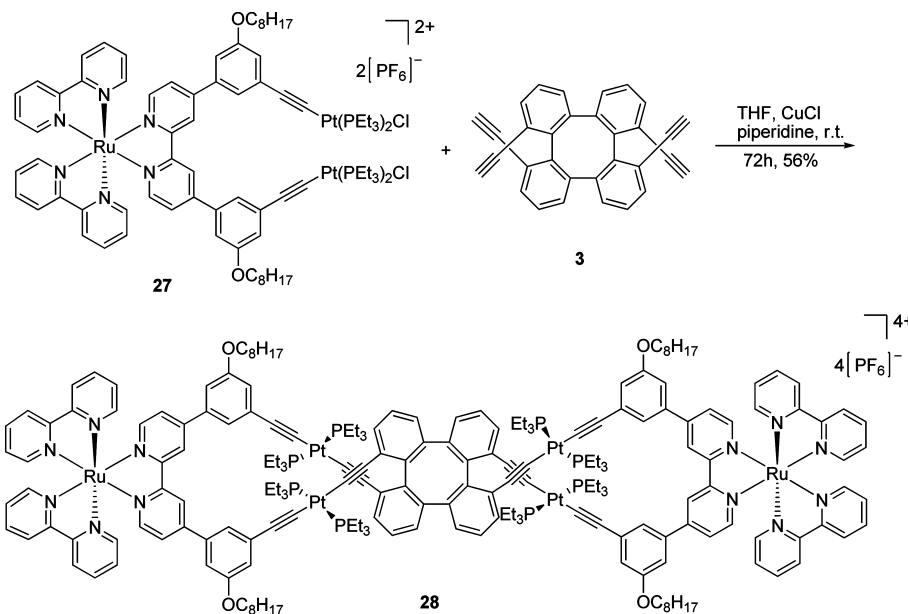


Figure 9. CD spectra of (*R,R*)-**3**, **15**, **28** and (*S,S*)-**3**, **15**, **28** in acetonitrile at concentrations of 1.0×10^{-5} M.

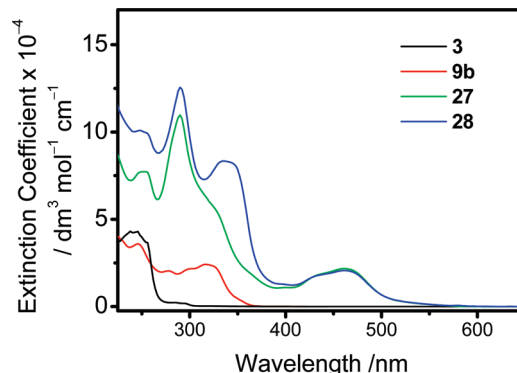


Figure 10. Electronic absorption spectra of selected compounds in acetonitrile at 298 K.

metal-to-ligand charge transfer (MLCT) transitions. The heterometallic platinum(II)-ruthenium(II) complexes **27** and **28** displayed similar electronic absorption spectra, in which there are higher-energy absorption bands at 290–334 nm and lower-energy absorption bands at 428–462 nm. The higher-energy absorption bands are attributed to the $\pi-\pi^*$ intraligand (IL)

Table 1. Photophysical Data of Selected Compounds in Acetonitrile at 298 K

Compound	Medium (T/K)	Absorption $\lambda_{\text{max}}/\text{nm}$ ($\epsilon_{\text{max}}/\text{dm}^3 \text{ mol}^{-1}\text{cm}^{-1}$)	Emission	
			$\lambda_{\text{max}}/\text{nm}$ ($\tau_0/\mu\text{s}$)	Φ_{em}^b
3	MeCN (298)	246 (42 970), 254 (36 830), 288 (2085)	— ^a	—
	Solid (298)			520 (<0.1)
	Solid (77)			488 (36.7)
	^a PrCN (77)			458 (43.7)
9b	MeCN (298)	246 (35 905), 278 (20 440), 300 (21 645), 320 (23 925)	430 (<0.1) 547 (<0.1) 490 (82.1) 455 (62.0)	$<10^{-3}$ ^c
	Solid (298)			547 (<0.1)
	Solid (77)			490 (82.1)
	^a PrCN (77)			455 (62.0)
27	MeCN (298)	254 (77 280), 290 (109 770), 326 sh (56 430), 428 (16 850), 462 (21 740)	621 (1.7) 623 (0.7) 625 (3.2) 594 (5.9)	13.9×10^{-2}
	Solid (298)			623 (0.7)
	Solid (77)			625 (3.2)
	^a PrCN (77)			594 (5.9)
28	MeCN (298)	248 (100 940), 290 (125 580), 334 (83 435), 428 (16 830), 462 (20 600)	621 (1.7) 625 (0.2) 623 (4.5) 595 (5.1)	8.6×10^{-2}
	Solid (298)			625 (0.2)
	Solid (77)			623 (4.5)
	^a PrCN (77)			595 (5.1)

^a Cannot be detected. ^b Luminescence quantum yield, measured at room temperature using $[\text{Ru}(\text{bpy})_3]^{2+}$ in degassed acetonitrile as a standard. ^c Too weak to be measured with great accuracy.

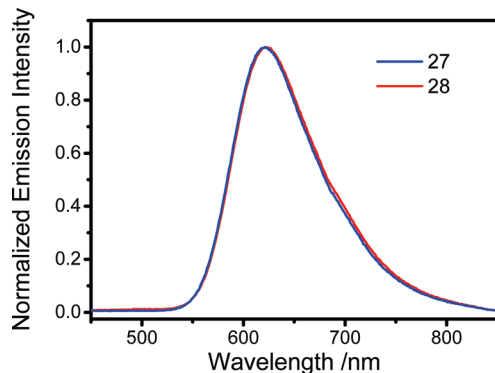


Figure 11. Emission spectra of **27** and **28** in degassed acetonitrile at 298 K.

transition of the polypyridyl and alkynyl ligands, with some mixing of $d\pi(\text{Pt}) \rightarrow \pi^*(\text{C}\equiv\text{CR})$ metal-to-ligand charge transfer (MLCT) transitions.²⁴ On the other hand, the lower-energy absorption bands at 428–462 nm, which are absent in the homometallic platinum(II) complexes, are assigned as a $d\pi(\text{Ru}) \rightarrow \pi^*(\text{bpy})$ metal-to-ligand charge transfer (MLCT) transition, typical of other ruthenium(II) polypyridyl complexes.²⁵ Upon photoexcitation, some of them showed intense emission for various media and temperatures. Complex **9b** showed emission at 430 nm in acetonitrile at 298 K, which is assigned to an origin of the metal-perturbed IL excited state. Upon excitation at $\lambda > 420$ nm, the heterometallic platinum(II)–ruthenium(II) complexes **27** and **28** exhibited an intense emission band at 621 nm in acetonitrile at 298 K (Figure 11), with large Stokes shifts and lifetimes in the microsecond range, which are indicative of their triplet parentage. On the basis of the characteristic emission observed at a similar energy in the well-studied ruthenium(II) tris(bipyridine) system,²⁵ together with the fact that the alkynylplatinum(II) phosphine complexes usually displayed emission at a relatively higher energy ($\lambda_{\text{em}} < 600$ nm), the origin of such an emission band at 621 nm is ascribed to the triplet $d\pi(\text{Ru}) \rightarrow \pi^*(\text{bpy})$ metal-to-ligand charge transfer (MLCT) excited state. Excitation at a higher energy ($\lambda = 340$ nm) yielded the same low-energy emission band. The excitation spectra of **27** and **28** closely resemble the corresponding electronic absorption spectra (Figure 10). The presence of the excitation band at 345 nm is

suggestive of an efficient energy transfer or internal conversion from the higher energy mixed $\pi-\pi^*$ intraligand (IL)/ $d\pi(\text{Pt}) \rightarrow \pi^*(\text{C}\equiv\text{CR})$ metal-to-ligand charge transfer (MLCT) excited state to the lowest-lying triplet $d\pi(\text{Ru}) \rightarrow \pi^*(\text{bpy})$ metal-to-ligand charge transfer (MLCT) excited state. Although the configuration of the platinum(II) metal centers in macrocycle **28** is preorganized or locked by the TETP bridging ligand in an inward direction, no observable metal–metal-to-ligand charge transfer (MMLCT) emission arising from the $\text{Pt}\dots\text{Pt}$ interaction could be found. It may probably be due to the presence of the sterically bulky triethylphosphine ligands, which prevent the two platinum(II) metal centers from coming into close proximity. On the other hand, the MMLCT excited state, even if it does exist in the heterometallic platinum(II)–ruthenium(II) complexes, would readily undergo energy transfer to the lowest-lying $d\pi(\text{Ru}) \rightarrow \pi^*(\text{bpy})$ metal-to-ligand charge transfer (MLCT) excited state, given its anticipated higher energy than the $d\pi(\text{Ru}) \rightarrow \pi^*(\text{bpy})$ MLCT state.

Conclusion

In this article, we report the synthesis of chiral 1,8,9,16-tetraethynyltetraphenylenne (**3**), which was employed as a chiral building block. Three types of chiral, helical, and rigid macrocycles were designed, whose chirality would be endowed by connecting with **3**. In this connection, three types of Pt(II) or Pt(II)–Ru(II) complexes **8**, **9b**, and **27** were initially prepared, which led to the formation of three designed helical assemblies **14**, **15**, and **28** via coordination-driven self-assembly, albeit the yield of **14** was very low. Their characterization was carried out by NMR and IR spectroscopy, ESI-MS spectrometry, and elemental analysis. Moreover, the CD spectra of these macrocycles also indicated chiral properties. Some of the platinum(II) and heterometallic platinum(II)–ruthenium(II) compounds were selected for photophysical study and were shown to exhibit interesting luminescence behavior. Emission characteristic of the lowest-lying triplet $d\pi(\text{Ru}) \rightarrow \pi^*(\text{bpy})$ MLCT excited state was observed in the heterometallic platinum(II)–ruthenium(II) compounds, while higher energy emission of a metal-perturbed

IL origin typical of platinum(II) alkynyl phosphines was observed in the homometallic platinum(II) species.

Acknowledgment. Dedicated to Professor Eiichi Nakamura on the occasion of his 60th birthday. The Institute of Molecular Functional Materials is an Area of Excellence under the University Grants Committee (Hong Kong). This work was supported by a grant from the Croucher Foundation (Hong Kong), a General Research Fund from Research Grants Council (Hong Kong) (RGC

ref. No. CUHK403909), the External Cooperation Program of the Chinese Academy of Sciences (BGrant No GJHZ200816), and the University Grants Committee Areas of Excellence Scheme (AoE/P-03/08). F.L. acknowledges with thanks the Croucher Foundation (Hong Kong) for a Shanghai Studentship. The Science and Technology Commission of the Shanghai Municipal Government also partially supported this program. We thank Professors Li-Xin Dai and Xue-Long Hou for helpful discussions.

Supporting Information Available: Experimental details, X-ray crystallographic data of **6**, **8**, and **9b**. This material is available free of charge via the Internet at <http://pubs.acs.org>. JA106599J

- (25) (a) Balzani, V.; Scandola, F. *Supramolecular Photochemistry*; Horwood: Chichester, U.K., 1990. (b) Denti, G.; Serroni, S.; Campagna, S.; Ricevuto, V.; Balzani, V. *Coord. Chem. Rev.* **1991**, *111*, 227–236. (c) Scandola, F.; Indelli, M. T.; Chiorboli, C.; Bignozzi, C. A. *Top. Curr. Chem.* **1990**, *158*, 73–149.